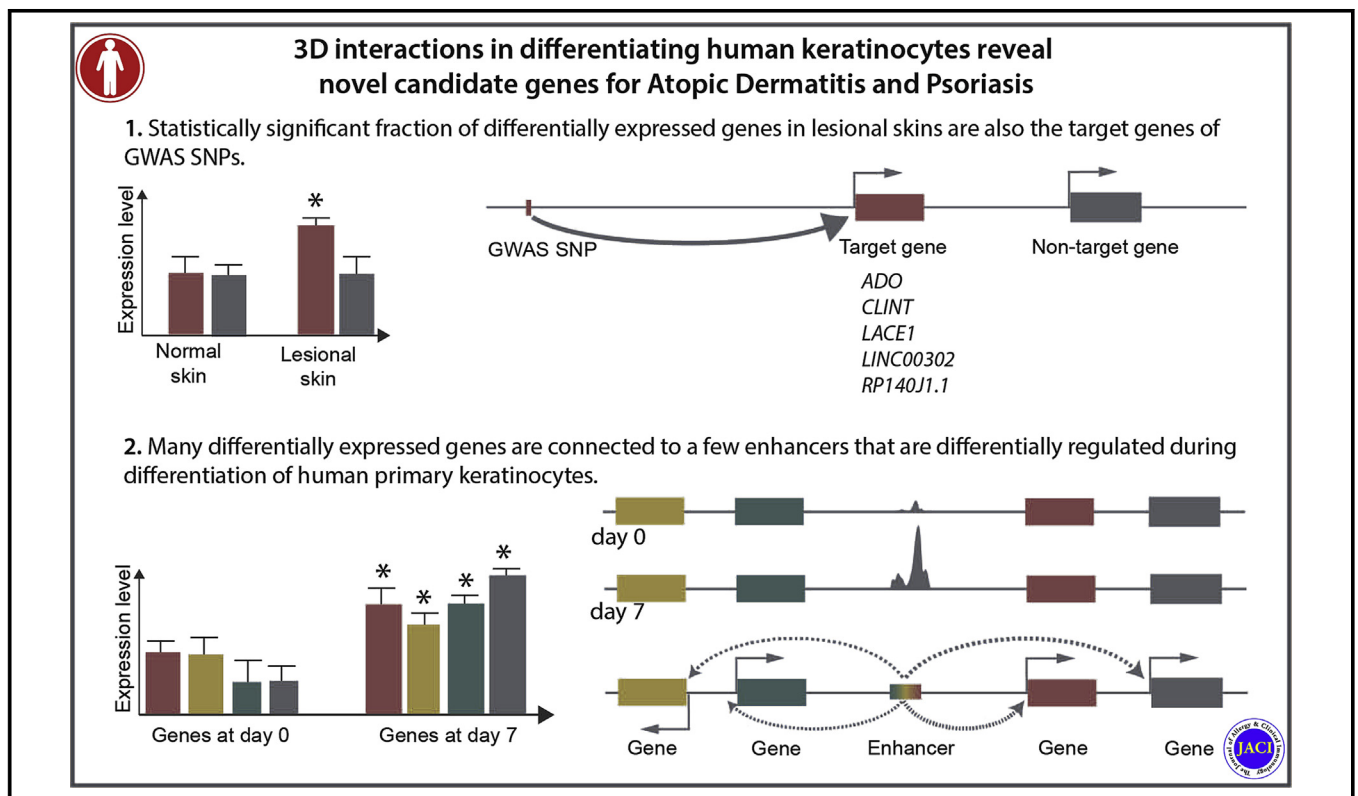


Chromatin interactions in differentiating keratinocytes reveal novel atopic dermatitis- and psoriasis-associated genes



Pelin Sahlén, PhD,^a Rapolas Spalinskas, PhD,^a Samina Asad, PhD,^b Kunal Das Mahapatra, MSc,^b Pontus Höjer, MSc,^a Anandashankar Anil, MSc,^a Jesper Eisfeldt, PhD,^{c,d} Ankit Srivastava, PhD,^b Pernilla Nikamo, PhD,^b Anaya Mukherjee, MSc,^b Kyu-Han Kim, PhD,^e Otto Bergman, PhD,^f Mona Stähle, MD, PhD,^b Enikő Sonkoly, MD, PhD,^{b,g,h} Andor Pivarcsi, PhD,^{b,h,i} Carl-Fredrik Wahlgren, MD, PhD,^b Magnus Nordenskjöld, MD, PhD,^{c,d} Fulya Taylan, PhD,^{c,d} Maria Bradley, MD, PhD,^{b,g*} and Isabel Tapia-Páez, PhD^{b*}
Stockholm, Solna, and Uppsala, Sweden; and Yongin-si, Korea

GRAPHICAL ABSTRACT



From ^athe KTH Royal Institute of Technology, School of Chemistry, Biotechnology and Health, Science for Life Laboratory, Stockholm; ^bthe Dermatology and Venereology Division, Department of Medicine Solna, ^cthe Department of Molecular Medicine and Surgery Center for Molecular Medicine and ^dthe Department of Cell and Molecular Biology, Karolinska Institutet, Stockholm; ^ethe Basic Research and Innovation Division, Research and Development Unit, AmorePacific Corporation, Yongin-si; ^fthe Division of Cardiovascular Medicine, Center for Molecular Medicine, Department of Medicine Solna, Karolinska Institutet, Stockholm, Karolinska University Hospital, Solna; ^gthe Department of Clinical Genetics, Karolinska University Hospital, Stockholm; ^hthe Department of Medical Biochemistry and Microbiology, Uppsala University, Uppsala; and ⁱthe Dermatology Unit, Karolinska University Hospital, Stockholm.

*These authors contributed equally to this work.

Supported by the Swedish Research Council (Vetenskapsrådet, grant 78081) and the Swedish Skin Foundation (grants 2544 and 2968). M.B. and I.T.P. received the Sanofi Genzyme Award for Type 2 Innovation Grant 2018 for this study. A.P. was funded by Swedish Skin Foundation (grants 2709 and 2948) and the Swedish Cancer Society (grant CAN 2018/801). The computations and data handling were made possible by

resources provided by the Swedish National Infrastructure for Computing at Rackham (UPPMAX), which was partially funded by the Swedish Research Council through grant agreement 2018-05973.

Disclosure of potential conflict of interest: The authors declare that they have no relevant conflicts of interest.

Received for publication April 17, 2020; revised August 14, 2020; accepted for publication September 17, 2020.

Available online October 16, 2020.

Corresponding author: Pelin Sahlén, PhD, Science for Life Laboratory, Tomtebodavägen 23A, 171 65, Stockholm, Sweden. E-mail: pelin.akan@scilifelab.se.

The CrossMark symbol notifies online readers when updates have been made to the article such as errata or minor corrections

0091-6749

© 2020 The Authors. Published by Elsevier Inc. on behalf of the American Academy of Allergy, Asthma & Immunology. This is an open access article under the CC BY license (<http://creativecommons.org/licenses/by/4.0/>).

<https://doi.org/10.1016/j.jaci.2020.09.035>

Background: Hundreds of variants associated with atopic dermatitis (AD) and psoriasis, 2 common inflammatory skin disorders, have previously been discovered through genome-wide association studies (GWASs). The majority of these variants are in noncoding regions, and their target genes remain largely unclear.

Objective: We sought to understand the effects of these noncoding variants on the development of AD and psoriasis by linking them to the genes that they regulate.

Methods: We constructed genomic 3-dimensional maps of human keratinocytes during differentiation by using targeted chromosome conformation capture (Capture Hi-C) targeting more than 20,000 promoters and 214 GWAS variants and combined these data with transcriptome and epigenomic data sets. We validated our results with reporter assays, clustered regularly interspaced short palindromic repeats activation, and examination of patient gene expression from previous studies.

Results: We identified 118 target genes of 82 AD and psoriasis GWAS variants. Differential expression of 58 of the 118 target genes (49%) occurred in either AD or psoriatic lesions, many of which were not previously linked to any skin disease. We highlighted the genes *AFG1L*, *CLINT1*, *ADO*, *LINC00302*, and *RPI-140J1.1* and provided further evidence for their potential roles in AD and psoriasis.

Conclusions: Our work focused on skin barrier pathology through investigation of the interaction profile of GWAS variants during keratinocyte differentiation. We have provided a catalogue of candidate genes that could modulate the risk of AD and psoriasis. Given that only 35% of the target genes are the gene nearest to the known GWAS variants, we expect that our work will contribute to the discovery of novel pathways involved in AD and psoriasis. (J Allergy Clin Immunol 2021;147:1742-52.)

Key words: Atopic dermatitis, psoriasis, Capture Hi-C, *AFG1L*, *CLINT1*, *ADO*, *LINC00302*, *RPI-140J1.1*

Atopic dermatitis (AD) and psoriasis are complex skin inflammatory diseases with several genetic components that interplay with environment factors¹ to cause disease resulting in a significant burden for affected individuals, families, and society. AD affects up to 20% of children and 3% to 5% of adults in the Western world,² whereas psoriasis affects approximately 2% of the European population.³

Genetic studies have shown that defects in the skin barrier are important underlying factors in AD. Loss-of-function mutations of the filaggrin (*FLG*) gene are the most important known risk factors for AD.⁴

FLG is located in the epidermal differentiation complex (EDC) in 1q21, a region containing genes important for differentiation and cornification of keratinocytes. Previous studies of psoriasis indicated that immune cell dysfunction is the main underlying cause of disease. Recently, a transcriptomic study of psoriatic keratinocytes revealed a significantly altered global expression profile, indicating the importance of keratinocytes in the pathology of psoriasis.⁵

Genome-wide association studies (GWASs) have transformed the landscape of complex disease genomics by allowing

Abbreviations used

AD:	Atopic dermatitis
ADO:	2-Aminoethanethiol dioxigenase
Capture Hi-C:	Targeted chromosome conformation capture
CRISPR:	Clustered regularly interspaced short palindromic repeats
DE:	Differentially expressed
EDC:	Epidermal differentiation complex
FDR:	False discovery rate
GWAS:	Genome-wide association study
H3K27Ac:	Histone 3 lysine 27 acetylation
Hi-C:	Genome wide chromosome conformation capture
LD:	Linkage disequilibrium
LINC:	Long intergenic noncoding
PIR:	Promoter interacting region
SAM:	Synergistic activation mediator system
sgRNA:	Single-guide RNA
SNP:	Single-nucleotide polymorphism
TF:	Transcription factor

identification of variants overrepresented in individuals with the disease of interest. At the time of study, 493 single-nucleotide polymorphisms (SNPs) associated with AD and psoriasis traits have been identified by using GWASs (downloaded from the European Bioinformatics Institute GWAS catalogue⁶ on August 22, 2018; association $P < 1e-6$), of which only 7% are in coding genes. Because the vast majority of these GWAS variants are non-coding, assigning causality is challenging. However, GWAS variants are enriched within enhancers (short DNA sequences that loop over several kilobases to come into proximity with promoters of their target genes to modulate their expression). Typically, the gene nearest to a GWAS variant is assigned as its target gene; however, only one-third of interactions actually involve the nearest gene.⁷⁻⁹

Recently, chromosome conformation capture coupled with next-generation sequencing (genome wide chromosome conformation capture [Hi-C]) has been used to map genomic looping and has proved instrumental to the study of large-scale genome structure. However, Hi-C lacks the resolution to map individual promoter-enhancer interactions. Therefore, we and others developed the targeted chromosome conformation capture (Capture Hi-C) methodology with improved resolution to investigate genomic interaction of only the targeted regions of interest, such as promoters, and hence to allow mapping of individual promoter-enhancer loops. Capture Hi-C has already been successfully used to study complex diseases such as schizophrenia,^{10,11} cardiovascular disease,⁹ autoimmune disease,¹² cancer,¹³ and heart failure.¹⁴ In this study, we have applied Capture Hi-C to primary human differentiating keratinocytes to identify variants and genes involved in the etiology of AD and psoriasis. We have integrated the promoter interaction maps with gene expression and histone enhancer mark data (histone 3 lysine 27 acetylation [H3K27Ac], a marker for enhancer regions) to map and prioritize GWAS target genes. We have also validated a number of enhancer variants by using gene reporter and clustered regularly interspaced short palindromic repeats (CRISPR) activation assays and have proposed a set of novel susceptibility genes for AD and psoriasis.

METHODS

A full description of the study method and data analysis is available in the [Methods](#) section of the Supplementary Material in this article's Online Repository (available at www.jacionline.org).

Capture Hi-C

Capture Hi-C was performed according to the method described in Sahlén et al.¹⁵ Briefly, the method consists of (1) cross-linking of DNA-protein-DNA with formaldehyde, (2) digestion with restriction endonucleases that cut DNA into approximately 700-bp pieces across the genome, (3) ligation of spatially close fragments, (4) capture of promoter-enhancer sequences by using probes that are located in promoters of known genes and probes containing SNPs associated with AD and psoriasis, (5) high-throughput sequencing, and (6) analysis of sequence data for significant regulatory interactions. A detailed description of the protocol is available in the [Supplementary Material](#).

Cloning and luciferase assays

From the Capture Hi-C results we chose sequences containing AD- or psoriasis-associated SNPs that interact with promoters of interesting genes. PCR-amplified fragments in control DNA were cloned into the pGL3 promoter vector (Promega). The QuickChange II Site-Directed Mutagenesis kit (Agilent Technologies, Santa Clara, Calif) was used to obtain alternative variants of selected SNPs. Luciferase assays were performed in 293T cells. FuGene 6 (Promega, Madison, Wis) transfection was performed with Renilla luciferase and pGL3 promoter constructs or empty vectors. After 24 hours, the cells were harvested and luciferase expression was measured by dual-luciferase assay (Promega) in a GloMax 96-microplate luminometer as described earlier.¹⁶ Relative luciferase expression was normalized to Renilla luciferase expression, and the results have been presented as relative ratios.

CRISPR activation using the SAM system

The CRISPR/Cas9 synergistic activation mediator (SAM) system consisting of 3 plasmids—single-guide RNA (sgRNA) (MS2) cloning backbone, MS2-P65-HSF1_GFP, and dCAS9-VP64_GFP—were purchased from Addgene. Design of sgRNAs for RP1-140J1.1 targeted the region of interaction from Capture Hi-C analysis. Individual sgRNA expression plasmids were constructed according to the SAM target sgRNA cloning protocol.¹⁷ Correct insertion was verified by Sanger sequencing. Primary adult keratinocytes (passage 3) at 60% to 70% confluence were transfected with sgRNA (MS2), MS2-P65-HSF1_GFP, and dCAS9-VP64-GFP plasmids (100 ng of each plasmid per well in 24-well plates) with Lipofectamine 2000 (ThermoFisher Scientific, Waltham, Mass). The expression of RP1-140J1.1 was confirmed by quantitative RT-PCR. After screening in primary keratinocytes, sgRNAs that transcriptionally activated RP1-140J1.1 were subsequently used in a keratinocyte differentiation assay where the keratinocytes were first transfected with the SAM plasmids followed by differentiation for 48 hours in growth factor-depleted EpiLife (ThermoFisher Scientific) medium containing 1.5 mM calcium chloride.

RESULTS

Keratinocyte differentiation and quality control

We differentiated primary basal epithelial keratinocytes by using calcium and performed Capture Hi-C, RNA sequencing, and chromatin immunoprecipitation followed by sequencing—H3K27Ac at 3 time points—day 0 (before the addition of calcium), day 3, and day 7—in 2 replicates ([Fig 1, A](#)). We confirmed the success of keratinocyte differentiation by analyzing the profile of the differentially expressed (DE) genes at the 3 time points^{18,19} (see [Table E1](#) and [Fig E1, A-C](#) in this article's Online Repository at www.jacionline.org). Moreover, regions that changed H3K27Ac enhancer marks following differentiation were enriched for

transcription factors (TFs) relevant for differentiation ([Fig 1, B](#) and see [Fig E1, D-F](#)).^{20,21}

Interaction profile of differentiated keratinocytes

We then turned our attention to promoter interactions identified by using Capture Hi-C.¹⁵ We investigated the interaction profile of 21,479 promoters and 214 variants associated with AD and psoriasis (see [Table E2](#) in this article's Online Repository at www.jacionline.org). We chose to target all reported GWAS variants (association $P < 1e-6$) to include variants with weaker effects and detect as many regulatory partners of promoters as possible, because many promoters are regulated by multiple enhancers with varying effect sizes.²²⁻²⁴ We found 57,921 interactions between 9,224 promoters and 35,643 distal regions, as well as 12,026 interactions between 8,941 promoters (a minimum of 5 read pairs and $P < .01$ in both replicates; Bonferroni-corrected $P < .02$ [see the [Methods](#) section and [Table E3](#) in this article's Online Repository at www.jacionline.org]).²⁵ Interacting genes were expressed at higher levels (2-sample t test $P = 1.1e-165$) and were more likely to be DE at different time points (chi-square test $P = 1.01e-27$ [see [Fig E2, A-C](#) in this article's Online Repository at www.jacionline.org]). The interacting genes were enriched for relevant gene families such as genes containing EF-hand domains that bind to intracellular calcium and type I and II keratins (see [Fig E2, D](#)). We found that interacting promoters associated with the same enhancers (ie, shared enhancers) were more likely to be DE during differentiation ([Fig 1, C](#)), suggesting a coordinated and distal activation of DE genes. Because enhancers regulate their target genes via looping to reach their promoters, we investigated the enhancer potential of promoter interacting regions (PIRs). We found that 69.5% of the PIRs (33,341) overlapped with at least 1 enhancer peak, with 9.9-fold enrichment for enhancers (see [Table E1](#)). Moreover, PIRs interacting with multiple promoters were more likely to overlap with enhancer marks, suggesting that there is complex regulation of some promoters by multiple enhancers ([Fig 1, D-E](#)).

Promoter interactions in differentiated keratinocytes were previously reported.²⁶ In a study by Rubin et al,²⁶ promoter-distal interactions between bait and nonbait fragments with a false discovery rate (FDR) less than 0.01 were considered to be enhancer-promoter interactions if the nonbait fragment overlapped with an H3K27ac peak at any day of the time course. Our study used DpnII (4-cutter; theoretical mean fragment size 650 bases) to fragment the genome, whereas the Rubin et al²⁶ study used HindIII (6-cutter; theoretical mean fragment size 4,500 bases). [Fig E3, A](#) (available in this article's Online Repository at www.jacionline.org) shows the length distribution of promoter and distal regions between the 2 studies. Because both studies overlapped H3K27Ac peaks to distal fragments, the nonbait length distributions were similar whereas the bait (promoter) distributions were significantly different on account of the different modes of genome fragmentation used (909 vs 7,835 bases; t test $P < 2.2e16$). The Rubin et al²⁶ study reported 207,663 interactions occurring between 19,312 promoters and 56,831 distal regions (covering 288 Mb [9.6% of the genome]). In this study, we have reported 57,921 interactions occurring between 9,224 promoters and 35,643 distal regions (covering 64 Mb [2.1% of the genome]). Furthermore, the distal interacting regions reported in the Rubin et al study also showed elevated read coverage within those found in this study (see [Fig E3, B](#)).

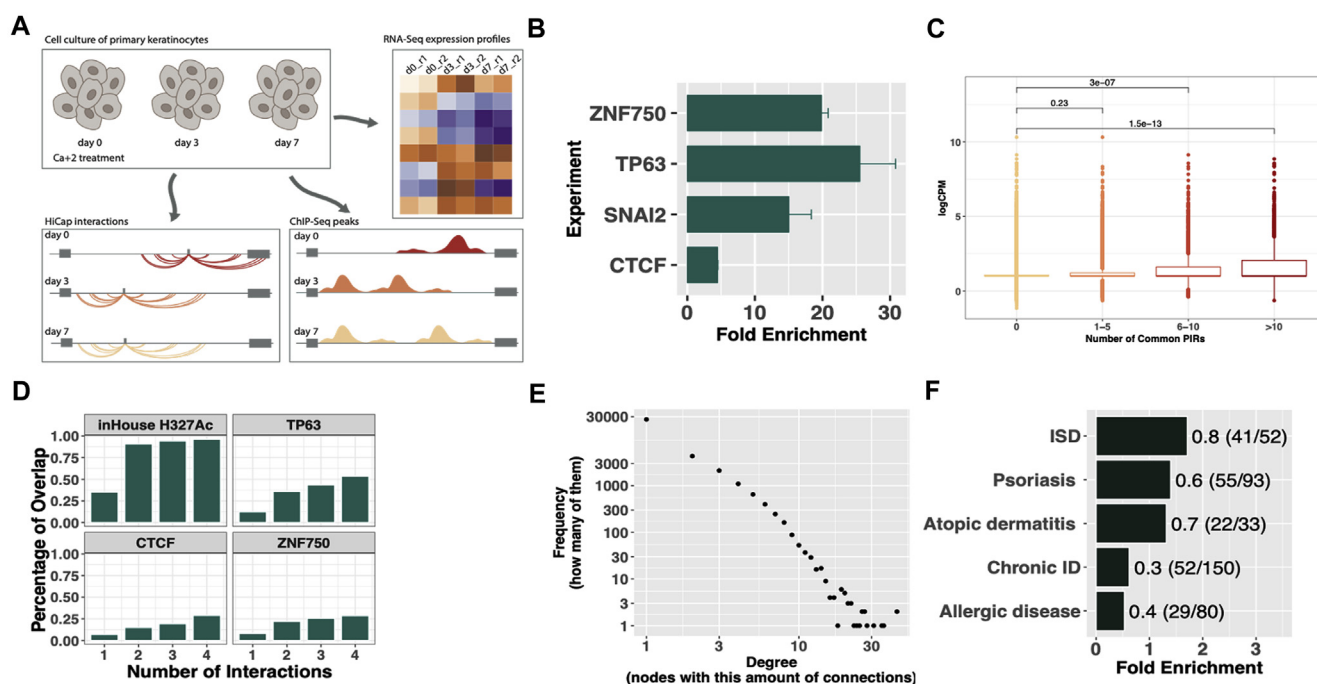


FIG 1. Complex regulatory landscape revealed by Capture Hi-C experiments on differentiated keratinocytes. **A**, Illustration of the experimental design. **B**, Differential H3K27Ac peaks (day 0 vs day 7) were enriched for TF binding sites relevant to keratinocyte differentiation and proliferation (see Table E1). **C**, Around 50% of the interacting promoters (6,051) shared a PIR. The shared number of PIRs correlated positively with their differential expression activity. **D**, Degree of distribution of PIRs, interactions from all time points combined. The x-axis denotes the number of connections of PIRs, and the y-axis denotes the number of PIRs with the corresponding amount of connections (ie, degree). On average, each PIR interacted with 1.63 promoters and each promoter interacted with 6.3 PIRs. **E**, Correlation between the number of promoters each PIR connects and the fraction of their overlap with an enhancer mark. **F**, Ratio of disease-associated variants with promoter interactions (see the Supplementary Material). Inflammatory skin disease (ISD), psoriasis, and AD were the top 3 traits enriched for interacting variants, whereas traits such as allergic disease were depleted (see Table E2, section 5.8). Only variants not targeted by capture probes were used in the analysis to avoid bias. ID, Inflammatory disease

Next, we counted GWAS SNPs (only those untargeted by Capture Hi-C probes in this study) with and without interactions to determine whether any trait or disease was enriched for interactions (see the Supplementary Material). Interestingly, in our setup the enriched traits for interactions were relevant to skin diseases (Fig 1, F and see the Supplementary Material).

We then looked at the interactions that changed significantly between time points. There were 3,686 dynamic interactions (6%) involving 1,693 genes that changed intensity (FDR < 0.1; absolute interaction support log-fold-change > 1.2) between any 2 time points (see Fig E4, A in this article's Online Repository at www.jacionline.org). Genes whose promoters had dynamic interactions were more likely to change their expression levels between the time points (2-sample *t* test; *P* = .00965). In addition, dynamic PIRs were enriched for binding sites for relevant TFs such as Krüppel-like factor 4 (*KLF4*), nuclear factor of activated T-cells 5 (*NFAT5*), SRY-box transcription factor 9 (*SOX9*), transcription factor AP-2 alpha (*TFAP2A*), YY1 transcription factor (*YY1*), tumor protein 63 (*TP63*), and forkhead box C1 (*FOXC1*) (Fig 2, A). PR/SET domain 1 gene (*PRDM1*),²⁷ a key repressor in cornification, showed a dynamic interaction profile and its promoter engaged in long-range interactions only at later stages of differentiation (Fig 2, B).

TF binding analysis of PIRs

Because TP63 is a significant player in terminal differentiation, we examined the interaction profile of PIRs overlapping with TP63 peaks in keratinocytes (TP63-PIRs). There were 10,306 promoter-distal interactions between 5,122 TP63-PIRs and 4,951 promoters, with an average interaction distance of 206 kilobases. To investigate the functional relevance of TP63-PIRs, we took only those genes that both interact with a TP63-PIR and show a minimum of 1.5-fold expression change between any 2 time points (FDR < 0.06, 346 genes) and performed a gene ontology overrepresentation analysis. We observed a strong enrichment for keratinocyte differentiation (Bonferroni-adjusted *P* = 1.86e-11), epidermis development (Bonferroni-adjusted *P* = 3.00e-15), cornified envelope (Bonferroni-adjusted *P* = 6.712e-10), and keratinization pathway (Bonferroni-adjusted *P* = 1.25e-6) (see Fig E4, B). Interestingly, when we performed the same analysis using the genes nearest to TP63-PIRs, we obtained only 2 relevant enriched terms, epidermis development and skin development (Bonferroni-adjusted *P* = 1.3e-5 and 1.16e-4, respectively), which confirms the power of 3-dimensional interaction maps in connecting putative enhancers to their target genes.

We also overlapped public zinc finger protein 750 (*ZNF750*) peaks in keratinocytes²⁸ with our data and found that 11% of our PIRs (3,659) overlapped with at least 1 *ZNF750* peak. Genes

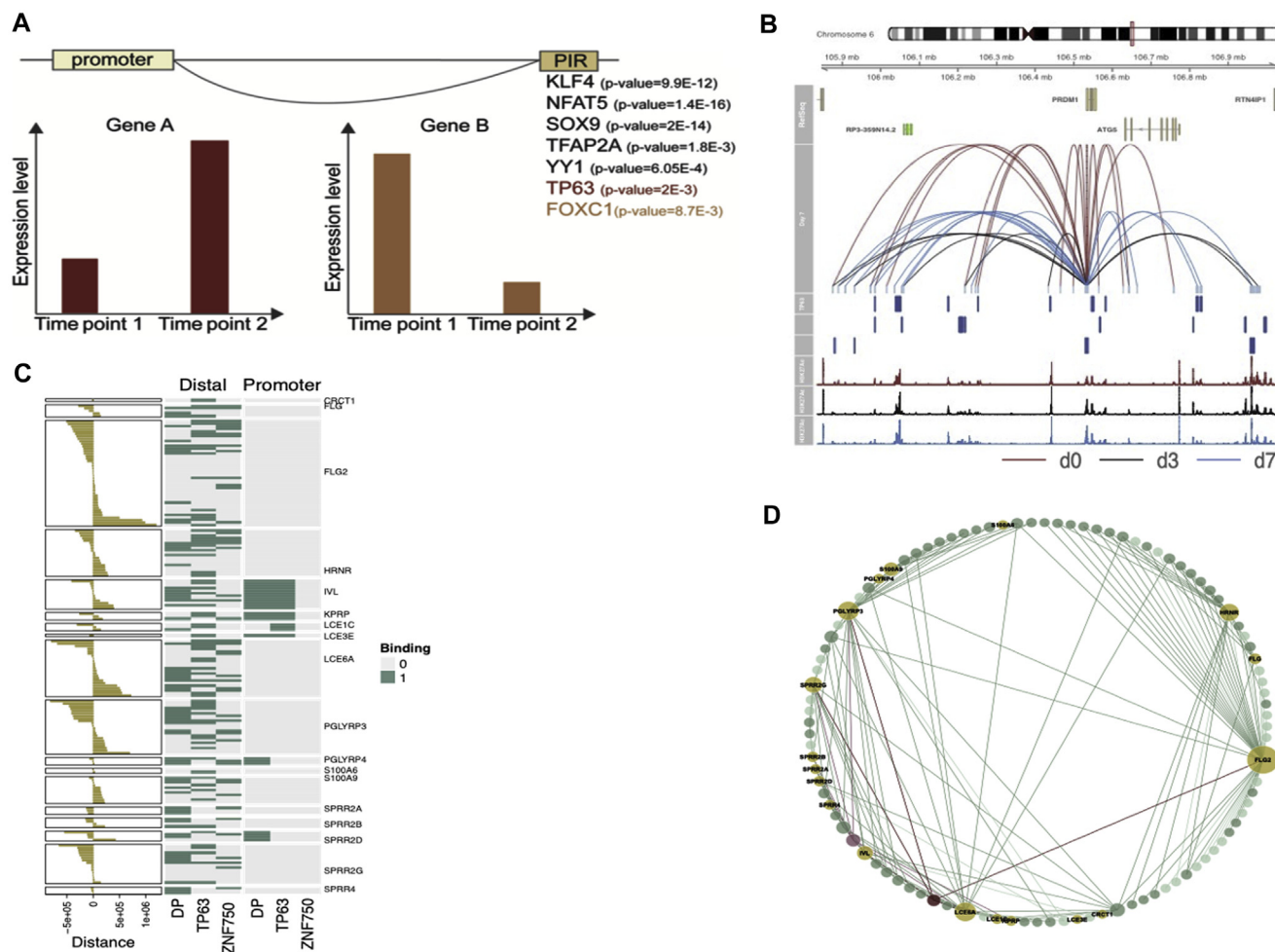


FIG 2. Interaction profile of the EDC region reveals coordinated regulation. **A**, Dynamic PIRs were enriched for TFs relevant to keratinocyte differentiation and general and looping TFs. Those connected to downregulated genes were enriched for *FOXC1*, and those connected to upregulated genes were enriched for TP63 motifs. **B**, Interactions of *PRDM1* spanning 1.1 Mb. The last 3 columns show H3K27Ac signal. The 3 tracks below the interaction track show *TP63*, *ZNF750*, and *CTCF* sites in keratinocytes. **C**, Promoter and enhancer states of DE genes in the EDC region, with respect to differential H3K27Ac signal (DP) and *TP63* and *ZNF750* binding events. Green indicates binding; yellow indicates no binding. Left bar plot denotes the interaction distance. **D**, In all, 36 PIRs interacted with more than 1 DE gene. Green and light green dots mark distal regions overlapping or not overlapping with enhancer marks, respectively. Yellow dots mark DE genes. The size of the dots correlates with their number of connections (ie, degree). Only nodes with more than 3 interactions are drawn for the sake of clarity. One PIR (chromosome 1 [chr1]: 152904024-152908609 [pink]) with a differential H3K27Ac and *ZNF750* peak connected to 9 DE genes. Another PIR (chr1: 152827325-152831779 [red]), containing differential H3K27Ac *TP63* peak, was connected to 7 DE genes.

connected to ZNF750-PIRs were enriched for pathways and processes such as keratinization (Bonferroni-adjusted $P = 1.4\text{e-}6$), formation of the cornified envelope (Bonferroni-adjusted $P = 5.5\text{e-}4$), and keratinocyte differentiation (Bonferroni-adjusted $P = 1.5\text{e-}9$). Only 28% of the ZNF750-PIRs were connected to their nearest genes. For example, 11 of the 14 genes that play a role in the process of establishment of skin barrier (GO:0061436) were connected to at least 1 ZNF750-PIR, and only 2 were the gene nearest to the ZNF750 peak (Table I).

A closer look at the EDC region

In the EDC region there were 474 promoter-distal interactions involving 52 promoters and 137 unique PIRs and 132 promoter-

promoter interactions involving 49 of the 58 expressed genes in the region (see Fig E5, A in this article's Online Repository at www.jacionline.org). Of the genes DE between the time points during calcium-induced differentiation, 84% (15 of 18) were connected to at least 1 differentially acetylated PIR during differentiation, whereas only 28% of these genes (5 of 18) were differentially acetylated at their promoters, providing support (chi-square $P = .0008$) for the enhancer-mediated regulation of differential expression by trans-acting factors (Fig 2, C). Table II lists the interactions of DE genes and their peak overlap profiles in the EDC locus. *In silico* analysis revealed that PIRs interacting with DE genes were enriched for KLF4 binding sites, a TF that activates late differentiation^{29,30} (binomial $P = 1.7\text{e-}223$ ³¹). Few enhancers were connected to many DE genes, suggesting

TABLE I. Genes associated with establishment of the skin barrier process (GO:0061436, 21 genes in total) and interacting with a ZNF750-PIR

Gene name	Gene symbol	Gene nearest to ZNF750-PIR?	Distance to ZNF750-PIRs
Claudin 4	<i>CLDN4</i>	No	16231 bp
Transmembrane serine protease 13	<i>TMPRSS13</i>	No	8,612 and 263,267 bp
Stratifin	<i>SFN</i>	No	278,368 bp
Keratin 1	<i>KRT1</i>	No	176,613 bp
Tumor protein p63	<i>TP63</i>	No	11,068 and 487,189 bp
Grainyhead like transcription factor 3	<i>GRHL3</i>	No	36,546 bp
Claudin 1	<i>CLDN1</i>	Yes	93,438 bp
ATP binding cassette subfamily A member 12	<i>ABCA12</i>	Yes	19,466, 37,560, and 154,885 bp
Arachidonate lipoxygenase 3	<i>ALOXE3</i>	No	103,249 and 205,847 bp
Hornerin	<i>HRNR</i>	No	38,721, 340,346, and 256,389 bp
Filaggrin family member 2	<i>FLG2</i>	No	8 regions; 6,386 to 502,642 bp distance
Keratinocyte differentiation factor 1	<i>KDF1</i>	Yes	70,006,181,099, and 337,722 bp
Grainyhead like transcription factor 1	<i>GRHL1</i>	No	123,705 bp
Chymotrypsin like elastase family member 2A	<i>CELA2A</i>	No	161,295 bp

Only 2 of the 14 genes interacted with the nearest ZNF750-PIR.

coordinated regulation by a limited set of enhancers (Fig 2, D). For example, 1 PIR (chromosome 1: 152904024-152908609) with a differential H3K27Ac and ZNF750 peak was connected to 6 DE genes. Another PIR (chromosome 1: 152827325-152831779) containing a differential H3K27Ac and TP63 peak was connected to 6 DE genes. *FLG*, the major risk gene for AD in Europeans, was connected to 5 different PIRs, 3 of which were differentially acetylated and possessed TP63 and ZNF750 binding sites. Of the interactions in the EDC region, 94% were not dynamic (ie, established before the differentiation), confirming previous results for the importance of preestablished promoter-enhancer contacts.²⁶

Interaction profile of AD and psoriasis GWAS SNPs in human keratinocytes

We next looked at all the SNPs associated with traits related to skin inflammation through GWASs in the European Bioinformatics Institute GWAS catalogue (downloaded on August 22, 2018 [see the [Supplementary Material](#) and [Table E4](#) in this article's Online Repository at www.jacionline.org]).⁶ Of 717 such GWAS variants, 118 (16.4%) interacted with at least 1 promoter in our setup (interacting with 199 promoters) (see [Table E5](#) in this article's Online Repository at www.jacionline.org). Of note, only 30% of the interactions involved the nearest gene. We then looked at the variants that are GWASs in linkage disequilibrium (LD) within 20 kb of the 717 GWAS variants. This identified 186 additional variants (interacting with 161 promoters), 35% of which interacted with the nearest gene. In total, 42% of skin disease-relevant GWAS or GWAS-LD variants (304 of 717) interacted with 312 genes (Fig 3, A and see [Table E5](#)). Of these 304 variants, 82 were associated with the traits AD and psoriasis and interacted with promoters of 118 genes. Of the 304 variants, 252 (83%) overlapped with an enhancer in keratinocytes and 138 (45%) variants overlapped with a TP63 binding site in keratinocytes. Moreover, interacting variants were more enriched for enhancer marks and TP63-binding sites compared with the total PIR data set (Fig 3, B), and their target genes were enriched for processes relevant for keratinocyte function (see Fig E4, B and C and [Table E6](#) in this article's Online Repository at www.jacionline.org). We tested the enhancer activity of 20 such variants, of which 17 (85%)

affected promoter activity; we found that 7 of the variants tested also showed allele-specific activity (see Fig E6). The target genes of variants associated with AD or psoriasis showed very little overlap (4 of 118 [3.3%]), which is in line with different diseases and rare co-occurrence of the 2 diseases (Fig 3, C and D).

Candidate gene prioritization for AD and psoriasis

A recent study by Tsoi et al³² found hundreds of DE genes in AD and psoriatic skin lesions compared with in their normal counterparts. We looked at the extent of overlap between the target genes of GWAS variants assigned in this study and DE genes in skin lesions and found that approximately 30% (97; chi-square $P = .04$) and 35% (122; chi-square $P = .7$) of the GWAS target genes were DE in psoriasis or AD lesions, respectively. However, for the variants with differences in luciferase activity, the ratio of target DE genes in lesions was significantly higher; 49% (19 of 39; chi-square $P = 6.4E-5$) and 69% (27 of 39; chi-square $P = 4.2E-6$) in AD and psoriasis lesions, respectively, (Fig 4, A). In total, 33 genes were DE in skin lesions and also interacted with AD or psoriasis GWAS or GWAS-LD variants with differences in luciferase activity. Most of these genes (26 of 33 [78%]) have not previously been linked to either AD or psoriasis and thus require further investigation (Fig 4, A).

Uncharacterized LOC101928009 (*RP1-140J1.1*), a long intergenic noncoding RNA (lincRNA) gene, is DE in both AD and psoriatic lesions. Its promoter is the second most connected promoter within the EDC region, and it is expressed only in skin and testis.³³ It is also upregulated during differentiation and interacts with GWAS variants associated with both psoriasis and AD (Fig 4, A). CRISPR-mediated transcriptional activation of the *RP1-140J1.1* promoter resulted in significant overexpression of key keratinocyte genes such as *FLG*, involucrin (*IVL*), and lorcrin cornified envelope precursor protein (*LORICRIN*) (Fig 4, B). Further, the *RP1-140J1.1* promoter carries an enhancer mark in keratinocytes³⁴ and could function as an enhancer-promoter (ePromoter).³⁵

Long intergenic nonprotein coding RNA 302 (*LINC00302*), a poorly studied lincRNA in the EDC region, is expressed almost exclusively in the skin³³ and is upregulated in late differentiated keratinocytes. *LINC00302* is downregulated in AD lesions but

TABLE II. Interacting regions of DE genes in the EDC region (chr1, 151,972,910-153,642,037, hg19 assembly)

Interacting gene	PIR	Distance	H3K27Ac peak D0 vs D3	H3K27Ac peak D0 vs D3	RPKM D0	RPKM D3	RPKM D7	TF binding
<i>FLG</i>	chr1: 152160951-152165378	135,574	-1.7	-1.35	3.0	6.1	28.0	TP63, CTCF
<i>FLG</i>	chr1: 152222132-152226238	-75,547	1	1	3.0	6.1	28.0	—
<i>FLG</i>	chr1: 152413913-152417549	116,234	-1.97	-1.8	3.0	6.1	28.0	—
<i>LCE6A</i>	chr1: 152712060-152714295	-103,269	1	1	3.5	2.6	161.6	TP63
<i>LCE6A</i>	chr1: 152714672-152716036	-100,657	0	0	3.5	2.6	161.6	ZNF750
<i>LCE6A</i>	chr1: 152716036-152718584	-99,293	1	1	3.5	2.6	161.6	CTCF, ZNF750
<i>LCE1B</i>	chr1: 152716036-152718584	-68,410	1	1	0.9	0.9	15.8	CTCF, ZNF750
<i>LCE6A</i>	chr1: 152792843-152793429	-22,486	0	0	3.5	2.6	161.6	—
<i>LCE6A</i>	chr1: 152818005-152820587	2,676	1	1	3.5	2.6	161.6	TP63
<i>SPRR2G</i>	chr1: 152827325-152831779	-296,102	1	1	13.3	169.7	1310.3	TP63
<i>LCE6A</i>		11,996	1	1	3.5	2.6	161.6	TP63
<i>LCE1A</i>		27,377	1	1	1.6	4.0	128.6	TP63
<i>LCE1B</i>		42,879	1	1	0.9	0.9	15.8	TP63
<i>LCE1C</i>		48,218	1	1	6.8	6.0	42.7	TP63
<i>LCE1F</i>		78,478	1	1	2.2	1.7	48.1	TP63
<i>KPRP</i>		96,820	1	1	10.5	32.3	250.9	TP63
<i>LCE2A</i>		156,486	1	1	0.6	0.0	15.8	TP63
<i>LCE6A</i>	chr1: 152839238-152842510	23,909	0	0	3.5	2.6	161.6	CTCF
<i>SPRR2G</i>	chr1: 152843648-152845442	-279,779	1	1	13.3	169.7	1310.3	CTCF
<i>LCE6A</i>	chr1: 152843648-152845442	28,319	1	1	3.5	2.6	161.6	CTCF
<i>SPRR2G</i>	chr1: 152855470-152861758	-267,957	1.8	1	13.3	169.7	1310.3	TP63
<i>LCE6A</i>		40,141	1.8	1	3.5	2.6	161.6	TP63
<i>LCE1B</i>		71,024	1.8	1	0.9	0.9	15.8	TP63
<i>SPRR2G</i>	chr1: 152873323-152875416	-250,104	-1.4	-1.37	13.3	169.7	1310.3	—
<i>LCE6A</i>	chr1: 152873323-152875416	57,994	-1.4	-1.37	3.5	2.6	161.6	—
<i>SPRR2G</i>	chr1: 152904024-152908609	-219,403	-4.42	-4.71	13.3	169.7	1310.3	ZNF750
<i>SPRR2B</i>		-140,060	-4.42	-4.71	15.2	348.9	822.4	ZNF750
<i>SPRR2A</i>		-125,964	-4.42	-4.71	29.0	513.1	1095.4	ZNF750
<i>SPRR2D</i>		-109,570	-4.42	-4.71	80.9	2472.2	4278.3	ZNF750
<i>LCE6A</i>		88,695	-4.42	-4.71	3.5	2.6	161.6	ZNF750
<i>KPRP</i>		173,519	-4.42	-4.71	10.5	32.3	250.9	ZNF750
<i>LCE1F</i>	chr1: 152904024-152908977	155,177	-4.42	-4.71	2.2	1.7	48.1	ZNF750
<i>SPRR2G</i>	chr1: 152917942-152922588	-205,485	1.72	1.74	13.3	169.7	1310.3	—
<i>SPRR2B</i>		-126,142	1.72	1.74	15.2	348.9	822.4	—
<i>SPRR2A</i>		-112,046	1.72	1.74	29.0	513.1	1095.4	—
<i>SPRR2D</i>		-95,652	1.72	1.74	80.9	2472.2	4278.3	—
<i>LCE6A</i>		102,613	1.72	1.74	3.5	2.6	161.6	—
<i>LCE1C</i>		138,835	1.72	1.74	6.8	6.0	42.7	—
<i>SPRR2A</i>	chr1: 152938522-152942875	-91,466	-2.9	-3.06	29.0	513.1	1095.4	SNAI2
<i>SPRR2G</i>	chr1: 153094091-153097228	-29,336	1	1	13.3	169.7	1310.3	SNAI2, ZNF750
<i>SPRR2G</i>	chr1: 153098092-153101431	-25,335	1	1	13.3	169.7	1310.3	—
<i>SPRR2B</i>	chr1: 153098092-153101431	54,008	1	1	15.2	348.9	822.4	—
<i>S100A9</i>	chr1: 153335989-153339183	5,660	-2.43	-2.39	45.9	73.8	449.8	ZNF750
<i>LCE6A</i>	chr1: 153335989-153339183	520,660	-2.43	-2.39	3.5	2.6	161.6	ZNF750
<i>S100A16</i>	chr1: 153356637-153361040	-229,007	1	1	73.6	135.9	86.6	TP63
<i>S100A16</i>		-225,194	1	1	73.6	135.9	86.6	TP63
<i>S100A9</i>		26,308	1	1	45.9	73.8	449.8	TP63
<i>LCE6A</i>		541,308	1	1	3.5	2.6	161.6	TP63
<i>S100A9</i>	chr1: 153462097-153465016	131,768	1	-1.17	45.9	73.8	449.8	SNAI2
<i>S100A9</i>	chr1: 153465111-153467732	134,782	1	1	45.9	73.8	449.8	TP63, CTCF
<i>S100A16</i>	chr1: 153479092-153481419	-102,739	1.83	2.4	73.6	135.9	86.6	—
<i>S100A9</i>	chr1: 153479092-153481419	148,763	1.83	2.4	45.9	73.8	449.8	—
<i>S100A16</i>	chr1: 153486321-153489863	-99,323	1	1	73.6	135.9	86.6	ZNF750
<i>S100A16</i>	chr1: 153486321-153489863	-95,510	1	1	73.6	135.9	86.6	ZNF750
<i>S100A9</i>	chr1: 153486321-153489863	155,992	1	1	45.9	73.8	449.8	ZNF750
<i>S100A16</i>	chr1: 153543995-153548126	-41,649	1	1	73.6	135.9	86.6	CTCF
<i>S100A16</i>	chr1: 153543995-153548126	-37,836	1	1	73.6	135.9	86.6	CTCF
<i>S100A9</i>	chr1: 153543995-153548126	213,666	1	1	45.9	73.8	449.8	CTCF

chr1, Chromosome 1.

Interacting regions that do not overlap with any TF peak or H3K27Ac signal are not shown.

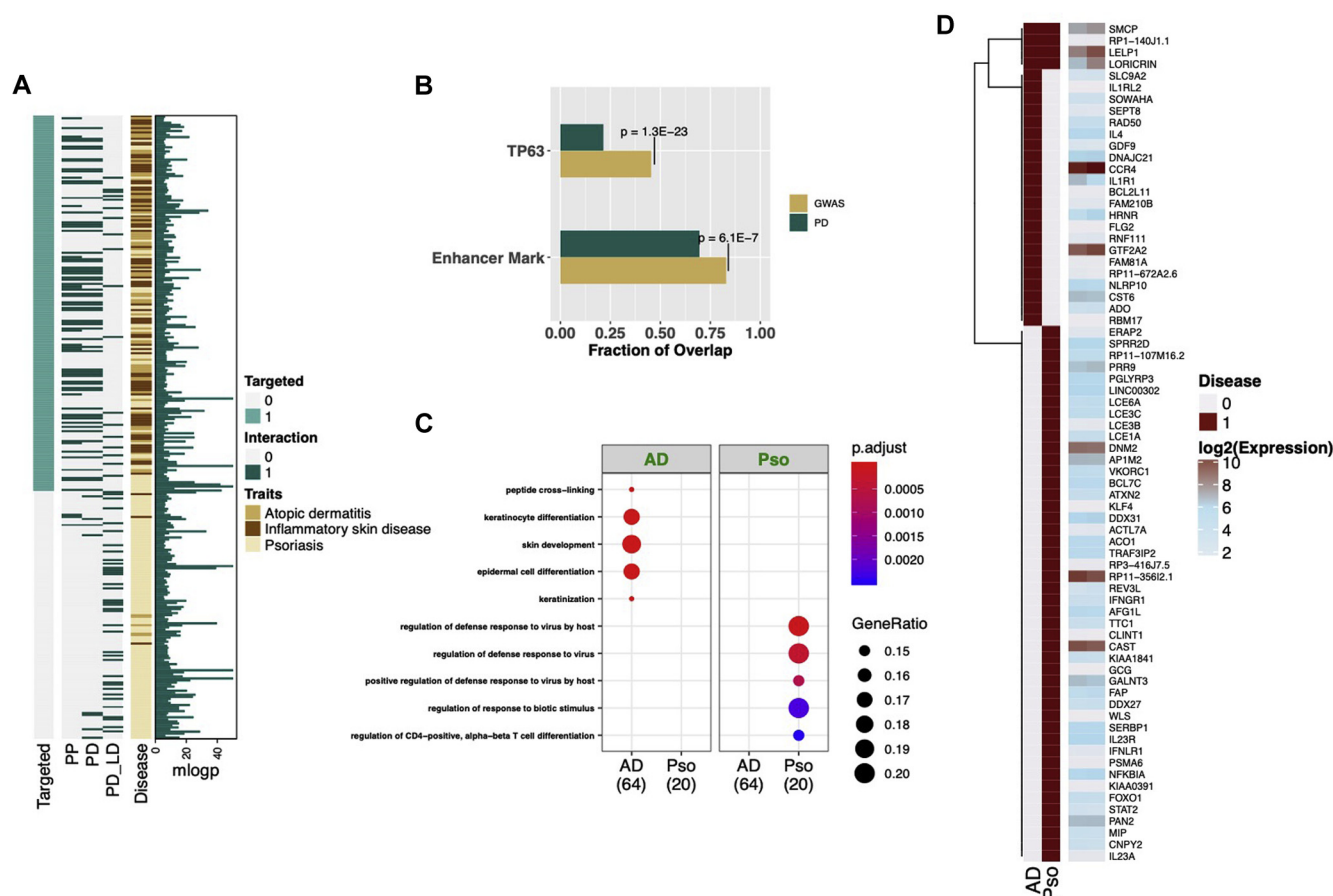


FIG 3. Genes connected to associated variants provide insight into pathways involved in skin diseases. **A**, Interaction status of all 717 GWAS variants. Targeted indicates whether a probe was designed for the GWAS variant. **B**, PIRs overlapping LD-expanded GWAS variants (717) were more enriched for TP63 binding sites and H3K27Ac marks than was the total PIR data set (35,643). Of the 304 interacting variants, 83% (252) overlapped with either an enhancer mark in keratinocytes, and 45% (138) overlapped with a TP63 binding site in keratinocytes. **C**, Overrepresented gene ontology (GO) terms (biologic process) for target genes of GWAS variants associated with AD (left) or psoriasis (right). The analysis was done by using ClusterProfiler, where only the different GO terms are plotted. The *P* values were adjusted with the FDR method. **D**, The expression levels of genes interacting with GWAS variants associated with AD (left) or psoriasis (right). The expression values are taken from GTEx database.³³ The expression columns (right) show mean expression for each gene in unexposed (387 individuals [left]) and sun-exposed (423 individuals [right]) skin. PD, Promoter-distal where the distal region contains a GWAS SNP; PD_LD, promoter-distal where the distal region contains a variant in LD with a GWAS variant; PP, promoter-GWAS,

not in psoriatic lesions (Fig 4, C). Genotyping of the promoter variant rs41267636 in 2 cohorts of patients with AD from 2 different populations ($n = 623$ and $n = 159$) (see the Methods section) showed no association with AD, suggesting that larger cohorts with more stratified phenotypes might be needed (see Table E7 in this article's Online Repository at www.jacionline.org). In addition, it has been shown that knock-down of *LINC00302* (WO2018056580A1) in primary human keratinocytes affects the expression of *FLG*, *IVL*, and *LORICRIN*.³⁶

Another DE gene in psoriatic lesions is Clathrin interactor 1 (*CLINT1*) gene, which promotes the assembly of clathrin-coated vesicles and mediates their transport. Our data show the *CLINT1* promoter interacts with 2 psoriasis-associated GWAS variants, rs2082412-G³⁷ (psoriasis, $P = 2e-28$) and rs3213094-A^{38,39} (psoriasis, $P = 3e-26$) (Fig 4, C).

2-Aminoethanethiol dioxygenase (*ADO*), which produces an enzyme expressed in skin, interacts with rs10995251⁴⁰ (AD, $P = 6e-20$) and is overexpressed in AD lesions.³²

The variant rs33980500-T^{41,42} (psoriasis, $P = 4e-45$), overlapping with the TP63 binding site, interacts with 3 genes: AFG1-like ATPase (*AFGIL*) (3.2 Mb away); TRAF3-interacting protein 2 (*TRAF3IP2*) (14.2 kb away); and REV3-like, DNA directed polymerase zeta catalytic subunit (*REV3L*) (108 kb away). *AFGIL* is DE in psoriatic lesions and rs33980500-T showed enhancer activity in a luciferase assay (see Fig E7). Coding variants within *TRAF3IP2* were previously found to be associated with psoriasis.⁴³ *REV3L* is an enzyme involved in the DNA damage response, and knockout of Rev3l in mice impairs wound healing in the epidermis and proliferation.⁴⁴

A 1.5-kb region in LD with the rs6677595-T⁴¹ variant (psoriasis, $P = 2e-33$; odds ratio = 1.26; 8 SNPs in LD, 1.7-2.9 kb away

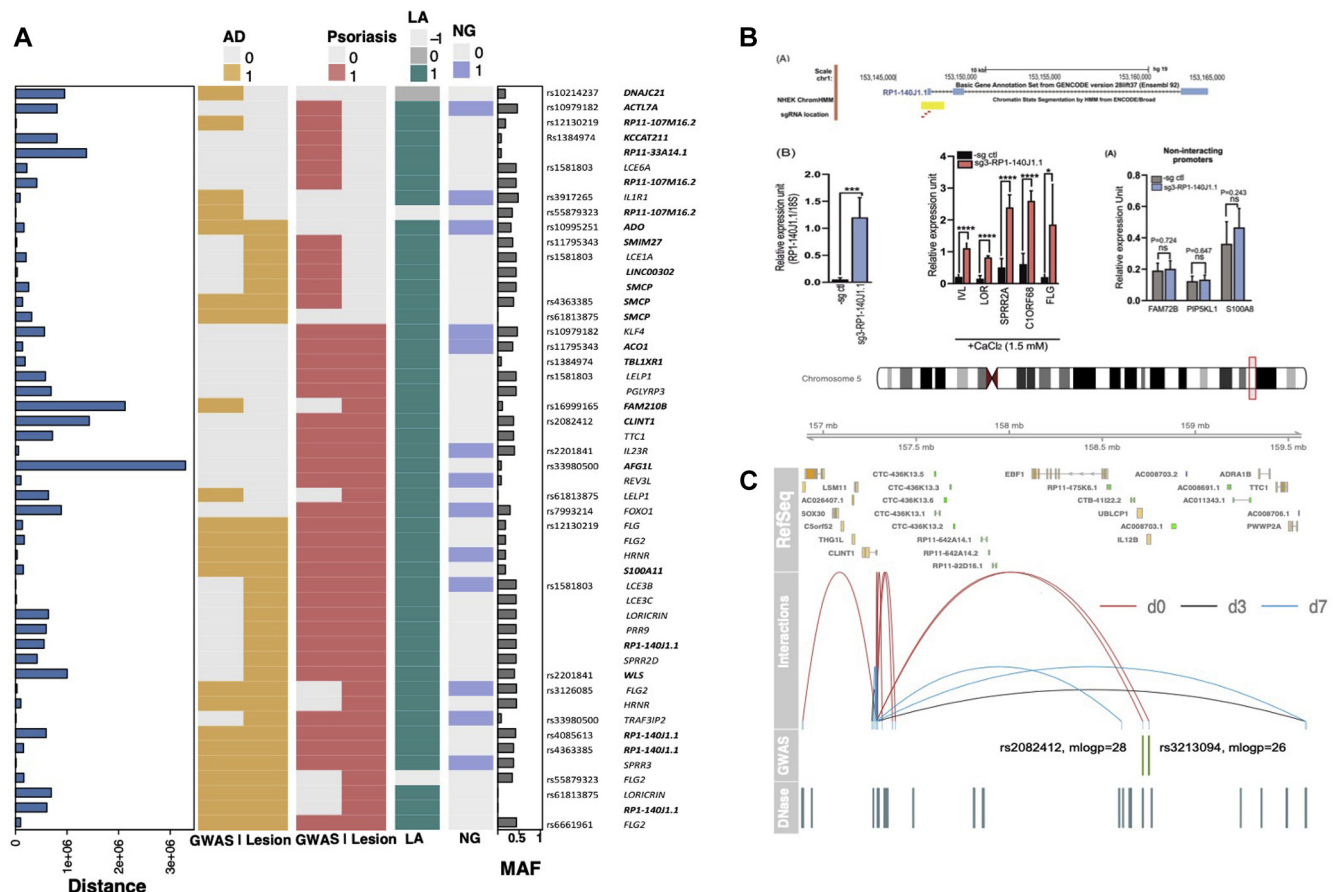


FIG 4. List of variants chosen for validation of Capture Hi-C interactions. **A**, (From left to right) Distance between GWAS SNP and promoter, AD GWASs, and AD lesions (yellow), psoriasis GWASs and psoriasis lesions (coral), luciferase activity (LA) (green), if the nearest gene (NG) (blue), minor allele frequency (MAF). The genes in bold are not associated with AD or psoriasis previously. **B**, (Top) *RP1-140J1.1* locus and the location of activating guide RNAs screened. ChromHMM³⁴ signal for *RP1-140J1.1* promoter is an active enhancer, as denoted by the yellow box (normal human epidermal keratinocyte [NHEK] ChromHMM track). (Bottom from left to right) Expression level of *RP1-140J1.1* in keratinocytes transfected with sgRNA3. The expression of several genes interacting with the promoter of *RP1-140J1.1* are upregulated by activation of *RP1-140J1.1* (black vs red). Other noninteracting promoters are shown (gray/blue), and none seems to be affected by *RP1-140J1.1* activation. * $P < .05$; *** $P < .001$; **** $P < .0001$; Student t test (representative of 2 independent replicates). **C**, Interactions of the *CLINT1* promoter spanning 2.4 Mb. GWAS panel shows rs2082412 and rs3213094, associated with psoriasis (mlogp = negative logarithm of association P value) and is located 1.43 and 1.46 Mb away from *CLINT1* promoter, respectively. The last column shows DNase-hypersensitive (HS) regions in human primary keratinocytes (chromatin immunoprecipitation [ChIP]-ATLAS).

from the index variant; $R^2 = 1$ [see Table E5]) was connected to promoters of 13 genes, 3 of which were also DE between the time points during calcium-induced differentiation. Although this region does not contain any H3K27Ac, TP63, or ZNF750 peaks, it does contain 3 predicted, perfect-match KLF4 motifs.

Furthermore, we found interactions between NLR family pyrin domain containing 10 (*NLRP10*) and rs878860⁴⁰ (AD; $P = 2 \times 10^{-22}$), IL-4 (*IL4*), and 3 GWAS variants associated with AD (rs12188917⁴⁵ [$P = 4 \times 10^{-17}$; interaction with an LD-SNP 1.9 kb away from the index variant rs3091307; $R^2 = 0.98$], rs4705962⁴⁵ [$P = 7 \times 10^{-12}$; interaction with an LD-SNP, 8.5 kb away from index variant rs35081016; $R^2 = 0.88$], and rs2897442⁴⁵ [$P = 4 \times 10^{-8}$]); both *NLRP10* and *IL4* played a role in regulation of T_H17 -type immune response. Confirming our findings, a recent study also identified rs878860 as residing within an enhancer that modulates the expression of *NLRP10*

gene, which functions as a suppressor of inflammation.⁴⁶ It should be noted that in the current study, level of *NLRP10* expression was found to be elevated during differentiation (log₂ fold change = 2.7; FDR = 0.06) and its promoter was found to interact with 2 regions (262 kb and 95 kb away), both overlapping TP63 and ZNF750 peaks in keratinocytes.

Genes that function in formation of cornified envelope, *FLG2*, hornerin (*HRNR*), late cornified envelope like proline rich 1 (*LELP1*), and *LORICRIN*, were connected to 4 AD GWAS variants. With the exception of *LELP1*, all were DE during differentiation. Another variant in LD with rs6661961-T⁴⁷ (AD; $P = 9 \times 10^{-11}$; variant in LD:rs17597997, 9.4 kb away from index variant; $R^2 = 0.97$) interacts with filaggrin family member 2 (*FLG2*) only during late differentiation and overlaps with the TP63 binding site. The genotype of rs6661961 is correlated with *FLG* expression in lymphoblastoid cell lines⁴⁷; however, with

our assay we did not detect any interaction with *FLG*. Further, the rs3126085-A⁴⁸ variant (AD, $P = 6e-12$; odds ratio = 1.22) was found to interact with the *HRNR* gene (104 kb away) and overlap with the DNase HS site, suggesting a regulatory role.

We also found that 3 genes, Wnt ligand secretion mediator (*WLS*), NFκB inhibitor alpha (*NFKBIA*), and ERBB receptor feedback inhibitor 1 (*ERRF1*), are associated with flaky skin phenotype (MP:0001195) in mice and interact with 5 psoriatic risk variants (see Table E5). None of these were the gene nearest to the risk variants.

DISCUSSION

Previous attempts to identify susceptibility genes for AD and psoriasis have involved familial and population studies, as well as transcriptome profiling. However, the genes identified thus far explain only a modest proportion of the heritability. The list of psoriasis- and AD-associated genomic variants has increased in recent years, mainly through GWASs.⁴⁹ For the majority of these variants, the target genes have not been identified, and because most are located in noncoding regions, the identification of their target genes is difficult. In this study we have used Capture Hi-C to identify new susceptibility genes for AD and psoriasis. Although several models relevant for AD and psoriasis could be used for this, such as immune cells or 3-dimensional models of skin, we chose a simple 2-dimensional cell culture model of human primary keratinocytes under differentiation. Using this model, we looked at the promoters that interact with relevant GWAS risk variants to identify their target genes. One such gene is a noncoding RNA gene, *LINC00302*, that interacts with psoriasis risk variants and when knocked down (WO2018056580A1) in primary human keratinocytes affected the expression of *FLG*, *IVL*, and *LORICRIN*.³⁶ Recently, it has also been shown that *LINC00302* is downregulated following thermal injury of dermis.⁵⁰ Future studies will be required to further establish the role of *LINC00302* in keratinocyte differentiation and pathogenesis. In addition, *CLINT1* interacts with psoriasis risk variants, and its knockdown in zebrafish results in psoriasis-like phenotypes such as leukocyte infiltration and excessive epithelial proliferation.⁵¹ Further, a *CLINT1* risk variant was shown to correlate with increased IL12B levels in peripheral blood samples from individuals with chronic plaque psoriasis.⁵² This suggests that this variant may contribute to disease risk in multiple tissues by regulating different risk genes. Also in this study, the ADO enzyme, which is expressed in skin and converts cysteamine to hypotaurine, an intermediate in the biosynthesis of taurine,⁵³ was found to be connected to a strong AD risk variant. Taurine is an essential compound for keratinocyte hydration and for protection of keratinocytes from osmotically and UV-induced apoptosis,^{53,54} *AFGIL*, which interacts with psoriasis risk variants, functions in mitochondrial protein homeostasis, and dysregulation of mitochondria may trigger inflammation and reduces apoptosis in keratinocytes.⁵⁵ Thus, these GWAS risk variants interact with promoters of genes found to be associated with skin diseases via functional studies, which confirms the relevance of our work in mapping target genes of risk variants. It is important to note that we included all reported GWAS variants in our analysis. Therefore, variant association strength (see Tables E4 and E5) should be taken into account during variant prioritization.

The dynamics of enhancer-promoter contact in epidermal keratinocyte differentiation was previously described by Rubin

et al.²⁶ A systematic comparison between our study and theirs reveals overlap between the interaction landscapes and good agreement between gene expression levels (see the [Supplementary Material](#)). Notably, we have reported a more dynamic interaction landscape than that reported by Rubin et al.²⁶ (6% vs 1.7%), and our approach targets promoters as well as GWAS SNPs, allowing for the functional assessment of GWAS SNPs and thus, the discovery of novel potential disease genes.

It is important to note that extensive linkage disequilibrium is not a major concern, in terms of isolating the causal/functional variant in our study, because only the causal variant will give an interaction signal if the causation is mediated by promoter looping, whereas the regions containing LD variants will give weaker or no interaction signal.

In summary, our study reveals that the majority of interactions in the EDC region are not dynamic (ie, established before the differentiation), confirming previous results for the importance of preestablished promoter-enhancer contacts.^{26,56,57} We have provided evidence for coordinated regulation of keratinocyte differentiation by a relatively small number of enhancers connected to several DE genes. Accordingly, several GWAS variants were found to connect to several genes, bringing into question the single gene association approach for each associated variant.^{58,59} We have listed genes DE in skin lesions that interact with GWAS variants, several of which have not been linked to AD or psoriasis before. The high confirmation rate of our findings through reporter assays and enrichment for dysregulated genes in lesions confirms the success of our approach in the identification of potential candidate genes.

Finally, we have highlighted *RP140J1.1*, *LINC00302*, *CLINT1*, *ADO*, and *AFGIL* for their potential functions in skin and as candidate genes for further investigation to understand the genetic etiology of skin diseases.

REFERENCES

1. Cookson WO. The genetics of atopic dermatitis: strategies, candidate genes, and genome screens. *J Am Acad Dermatol* 2001;45(suppl 1):S7-9.
2. Bos JD, Brenninkmeijer EE, Schram ME, Middelkamp-Hup MA, Spuls PI, Smitt JH. Atopic eczema or atopiform dermatitis. *Exp Dermatol* 2010;19:325-31.
3. Guttman-Yassky E, Krueger JG. Atopic dermatitis and psoriasis: two different immune diseases or one spectrum? *Curr Opin Immunol* 2017;48:68-73.
4. Damm A, Giebler N, Zamek J, Zigrino P, Kufer TA. Epidermal NLRP10 contributes to contact hypersensitivity responses in mice. *Eur J Immunol* 2016;46:1959-69.
5. Pasquali L, Srivastava A, Meisgen F, Das Mahapatra K, Xia P, Xu Landen N, et al. The keratinocyte transcriptome in psoriasis: pathways related to immune responses, cell cycle and keratinization. *Acta Derm Venereol* 2019;99:196-205.
6. Buniello A, MacArthur JAL, Cerezo M, Harris LW, Hayhurst J, Malangone C, et al. The NHGRI-EBI GWAS catalog of published genome-wide association studies, targeted arrays and summary statistics 2019. *Nucleic Acids Res* 2019;47:D1005-12.
7. Dostie J, Richmond TA, Arnaout RA, Selzer RR, Lee WL, Honan TA, et al. Chromosome conformation capture carbon copy (5C): a massively parallel solution for mapping interactions between genomic elements. *Genome Res* 2006;16:1299-309.
8. Gusev A, Ko A, Shi H, Bhatia G, Chung W, Penninx BW, et al. Integrative approaches for large-scale transcriptome-wide association studies. *Nat Genet* 2016;48:245-52.
9. Akerborg O, Spalinskas R, Pradhananga S, Anil A, Hojer P, Poujade FA, et al. High-resolution regulatory maps connect vascular risk variants to disease-related pathways. *Circ Genom Precis Med* 2019;12:e002353.
10. Pardinas AF, Holmans P, Pocklington AJ, Escott-Price V, Ripke S, Carrera N, et al. Common schizophrenia alleles are enriched in mutation-intolerant genes and in regions under strong background selection. *Nat Genet* 2018;50:381-9.
11. Rajarajan P, Borrmann T, Liao W, Schrodde N, Flaherty E, Casino C, et al. Neuron-specific signatures in the chromosomal connectome associated with schizophrenia risk. *Science* 2018;362.

12. Martin P, McGovern A, Orozco G, Duffus K, Yarwood A, Schoenfelder S, et al. Capture Hi-C reveals novel candidate genes and complex long-range interactions with related autoimmune risk loci. *Nat Commun* 2015;6:10069.
13. Baxter JS, Leavy OC, Dryden NH, Maguire S, Johnson N, Fedele V, et al. Capture Hi-C identifies putative target genes at 33 breast cancer risk loci. *Nat Commun* 2018;9:1028.
14. Arvanitis M, Tampakakis E, Zhang Y, Wang W, Auton A, and Me Research T, et al. Genome-wide association and multi-omic analyses reveal ACTN2 as a gene linked to heart failure. *Nat Commun* 2020;11:1122.
15. Sahlén P, Abdullayev I, Ramskold D, Matskova L, Rilakovic N, Lotstedt B, et al. Genome-wide mapping of promoter-anchored interactions with close to single-enhancer resolution. *Genome Biol* 2015;16:156.
16. Tapia-Paez I, Tammimies K, Massinen S, Roy AL, Kere J. The complex of TFII-I, PARP1, and SFPQ proteins regulates the DYX1C1 gene implicated in neuronal migration and dyslexia. *FASEB J* 2008;22:3001-9.
17. Konermann S, Brigham MD, Trevino AE, Joung J, Abudayyeh OO, Barcena C, et al. A genome-scale transcriptional activation by an engineered CRISPR-Cas9 complex. *Nature* 2015;517:583-8.
18. Watt FM, Green H. Stratification and terminal differentiation of cultured epidermal cells. *Nature* 1982;295:434-6.
19. Boyce ST, Ham RG. Calcium-regulated differentiation of normal human epidermal keratinocytes in chemically defined clonal culture and serum-free serial culture. *J Invest Dermatol* 1983;81(suppl 1):33s-40s.
20. Oki S, Ohta T, Shioi G, Hatanaka H, Ogasawara O, Okuda Y, et al. ChIP-Atlas: a data-mining suite powered by full integration of public ChIP-seq data. *EMBO Rep* 2018;19.
21. Davis CA, Hitz BC, Sloan CA, Chan ET, Davidson JM, Gabdank I, et al. The Encyclopedia of DNA Elements (ENCODE): data portal update. *Nucleic Acids Res* 2018;46:D794-801.
22. Chatterjee S, Kapoor A, Akiyama JA, Auer DR, Lee D, Gabriel S, et al. Enhancer variants synergistically drive dysfunction of a gene regulatory network in Hirschsprung disease. *Cell* 2016;167:355-68.e10.
23. Perry MW, Boettiger AN, Levine M. Multiple enhancers ensure precision of gap gene-expression patterns in the *Drosophila* embryo. *Proc Natl Acad Sci U S A* 2011;108:13570-5.
24. Malin J, Aniba MR, Hannehalli S. Enhancer networks revealed by correlated DNase hypersensitivity states of enhancers. *Nucleic Acids Res* 2013;41:6828-38.
25. Anil A, Spalinskas R, Akerborg O, Sahlén P. HiCapTools: a software suite for probe design and proximity detection for targeted chromosome conformation capture applications. *Bioinformatics* 2018;34:675-7.
26. Rubin AJ, Barajas BC, Furlan-Magaril M, Lopez-Pajares V, Mumbach MR, Howard I, et al. Lineage-specific dynamic and pre-established enhancer-promoter contacts cooperate in terminal differentiation. *Nat Genet* 2017;49:1522-8.
27. Magnusdottir E, Kalachikov S, Mizukoshi K, Savitsky D, Ishida-Yamamoto A, Panteleyev AA, et al. Epidermal terminal differentiation depends on B lymphocyte-induced maturation protein-1. *Proc Natl Acad Sci U S A* 2007;104:14988-93.
28. Boxer LD, Barajas B, Tao S, Zhang J, Khavari PA. ZNF750 interacts with KLF4 and RCOR1, KDM1A, and CTBP1/2 chromatin regulators to repress epidermal progenitor genes and induce differentiation genes. *Genes Dev* 2014;28:2013-26.
29. Segre JA, Bauer C, Fuchs E. Klf4 is a transcription factor required for establishing the barrier function of the skin. *Nat Genet* 1999;22:356-60.
30. Patel S, Xi ZF, Seo EY, McGaughey D, Segre JA. Klf4 and corticosteroids activate an overlapping set of transcriptional targets to accelerate in utero epidermal barrier acquisition. *Proc Natl Acad Sci U S A* 2006;103:18668-73.
31. Hartmann H, Guthohrlein EW, Siebert M, Luehr S, Soding J. P-value-based regulatory motif discovery using positional weight matrices. *Genome Res* 2013;23:181-94.
32. Tsoi LC, Rodriguez E, Degenhardt F, Baurecht H, Wehkamp U, Volks N, et al. Atopic dermatitis is an IL-13-dominant disease with greater molecular heterogeneity compared to psoriasis. *J Invest Dermatol* 2019;139:1480-9.
33. Consortium GT. The Genotype-Tissue Expression (GTEx) project. *Nat Genet* 2013;45:580-5.
34. Ernst J, Kellis M. ChromHMM: automating chromatin-state discovery and characterization. *Nat Methods* 2012;9:215-6.
35. Dao LTM, Galindo-Albarran AO, Castro-Mondragon JA, Andrieu-Soler C, Medina-Rivera A, Souaid C, et al. Genome-wide characterization of mammalian promoters with distal enhancer functions. *Nat Genet* 2017;49:1073-81.
36. Kim Gyu-han, Lee Tae-ryong, Cho Eun-gyeong, Sonui-dong, inventor. A composition for skin barrier function comprising LINC00302 promoting materials and a method for screening LINC00302 promoting materials. South Korea; 2016.
37. Nair RP, Duffin KC, Helms C, Ding J, Stuart PE, Goldgar D, et al. Genome-wide scan reveals association of psoriasis with IL-23 and NF-kappaB pathways. *Nat Genet* 2009;41:199-204.
38. Genetic Analysis of Psoriasis Consortium, the Wellcome Trust Case Control Consortium, Strange A, Capon F, Spencer CC, Knight J, et al. A genome-wide association study identifies new psoriasis susceptibility loci and an interaction between HLA-C and ERAP1. *Nat Genet* 2010;42:985-90.
39. Zhang XJ, Huang W, Yang S, Sun LD, Zhang FY, Zhu QX, et al. Psoriasis genome-wide association study identifies susceptibility variants within LCE gene cluster at 1q21. *Nat Genet* 2009;41:205-10.
40. Hirota T, Takahashi A, Kubo M, Tsunoda T, Tomita K, Sakashita M, et al. Genome-wide association study identifies eight new susceptibility loci for atopic dermatitis in the Japanese population. *Nat Genet* 2012;44:1222-6.
41. Tsoi LC, Spain SL, Knight J, Ellinghaus E, Stuart PE, Capon F, et al. Identification of 15 new psoriasis susceptibility loci highlights the role of innate immunity. *Nat Genet* 2012;44:1341-8.
42. Ellinghaus E, Ellinghaus D, Stuart PE, Nair RP, Debrus S, Raelson JV, et al. Genome-wide association study identifies a psoriasis susceptibility locus at TRA-F3IP2. *Nat Genet* 2010;42:991-5.
43. Huffmeier U, Uebe S, Ekici AB, Bowes J, Giardina E, Korendowycz E, et al. Common variants at TRAF3IP2 are associated with susceptibility to psoriatic arthritis and psoriasis. *Nat Genet* 2010;42:996-9.
44. Lange SS, Bhetawal S, Reh S, Powell KL, Kusewitt DF, Wood RD. DNA polymerase zeta deficiency causes impaired wound healing and stress-induced skin pigmentation. *Life Sci Alliance* 2018;1.
45. Paternoster L, Standl M, Waage J, Baurecht H, Hotze M, Strachan DP, et al. Multi-ancestry genome-wide association study of 21,000 cases and 95,000 controls identifies new risk loci for atopic dermatitis. *Nat Genet* 2015;47:1449-56.
46. Miyai M, Yamamoto-Tanaka M, Inoue K, Tsuboi R, Hibino T. Atopic dermatitis susceptible gene NLRP10 suppresses inflammatory reaction and NLRP10 SNP mutation down-regulates NLRP10 expression. *Journal of Dermatological Science* 2016;84:e69.
47. Weidinger S, Willis-Owen SA, Kamatani Y, Baurecht H, Morar N, Liang L, et al. A genome-wide association study of atopic dermatitis identifies loci with overlapping effects on asthma and psoriasis. *Hum Mol Genet* 2013;22:4841-56.
48. Sun LD, Xiao FL, Li Y, Zhou WM, Tang HY, Tang XF, et al. Genome-wide association study identifies two new susceptibility loci for atopic dermatitis in the Chinese Han population. *Nat Genet* 2011;43:690-4.
49. Loset M, Brown SJ, Saunes M, Hveem K. Genetics of atopic dermatitis: from DNA sequence to clinical relevance. *Dermatology* 2019;235:355-64.
50. Yu W, Guo Z, Liang P, Jiang B, Guo L, Duan M, et al. Expression changes in protein-coding genes and long non-coding RNAs in denatured dermis following thermal injury. *Burns* 2020;46:1128-35.
51. Dodd ME, Hatzold J, Mathias JR, Walters KB, Bennin DA, Rhodes J, et al. The ENTH domain protein Clint1 is required for epidermal homeostasis in zebrafish. *Development* 2009;136:2591-600.
52. Villarreal-Martinez A, Gallardo-Blanco H, Cerda-Flores R, Torres-Munoz I, Gomez-Flores M, Salas-Alanis J, et al. Candidate gene polymorphisms and risk of psoriasis: a pilot study. *Exp Ther Med* 2016;11:1217-22.
53. Grafe F, Wohlrab W, Neubert RH, Brandsch M. Functional characterization of sodium- and chloride-dependent taurine transport in human keratinocytes. *Eur J Pharm Biopharm* 2004;57:337-41.
54. Jancke G, Siefken W, Carstensen S, Springmann G, Bleck O, Steinhart H, et al. Role of taurine accumulation in keratinocyte hydration. *J Invest Dermatol* 2003;121:354-61.
55. Therianou A, Vasiadi M, Delivanis DA, Petrakopoulou T, Katsarou-Katsari A, Antoniou C, et al. Mitochondrial dysfunction in affected skin and increased mitochondrial DNA in serum from patients with psoriasis. *Exp Dermatol* 2019;28:72-5.
56. Atlasi Y, Megchelenbrink W, Peng T, Habibi E, Joshi O, Wang SY, et al. Epigenetic modulation of a hardwired 3D chromatin landscape in two naive states of pluripotency. *Nat Cell Biol* 2019;21:568-78.
57. Ghavi-Helm Y, Klein FA, Pakozdi T, Ciglar L, Noordermeer D, Huber W, et al. Enhancer loops appear stable during development and are associated with paused polymerase. *Nature* 2014;512:96-100.
58. Cannon ME, Mohlke KL. Deciphering the emerging complexities of molecular mechanisms at GWAS loci. *Am J Hum Genet* 2018;103:637-53.
59. Flister MJ, Tsai SW, O'Meara CC, Endres B, Hoffman MJ, Geurts AM, et al. Identifying multiple causative genes at a single GWAS locus. *Genome Res* 2013;23:1996-2002.